
**Detection of vegetation fraction from images
captured with low cost device**

Paulo Victor de Souza Prado



Contents

List of Figures	iii
List of Tables	v
1 Objective	1
2 Dataset	3
3 Steps	5
4 Results	7
References	11

List of Figures

2.1	Samples and ground truth	3
4.1	Example input image	7
4.2	Index result for the input example, in order up to right NGRDI, ExG, CIVE, VEG, ExGR and WI	7
4.3	Receiver Operating Characteristic (ROC) Curves	8
4.4	Example of filtered input (Blur, Mean, Gaussian and Bilinear)	9
4.5	NGRDI predictions	9
4.6	ROC curve for blurred input	10

List of Tables

4.1	Accuracy crop 1 and 2	8
4.2	Filter accuracy crop 1 and 2	9
4.3	Blurred crop1 database informations	10
4.4	Blurred crop 2 database informations	10

Listings

1 | Objective

Vegetation mapping is a crucial step for the development of the Precision Agriculture (PA) [4], which aims for a detailed management of the PA system.

The use of a low cost device makes it feasible to apply the method in developing countries, since the high cost related to some ways of image acquisition may be a barrier. To assist this research, an image database of bean plantations will be used, first explored in [2].

In this way we wish to detect the vegetation fraction of agricultural systems with a low cost of application. With this information the farmer can, in the future, obtain more specific information as: estimate of production and the presence of other vegetation rather than the one desired.

2 | Dataset

The dataset used in the project is formed by images of two bean plantations. Those images were captured by a Skyhook Helikite, with a camera Fujifilm Z20fd. The images are in PNG format with 24-bits RGB representation. All images were obtained from a height of 50 meters for both plantations, 63 days after the first appearance of the plants.

The images were cropped to form squares of 512 x 512 pixels. The dataset used contains 18 images of the first plantation, which is a more productive crop, and 22 images of the second plantation, which has a more scarce distribution, containing plants, herbs and soil.

For each one of the 40 images of the plantation, there is an equivalent image that contains the ground truth, constructed with the help of three agronomists who mapped whether a vegetation was present in regions of 16 x 16 pixels. So we ended up with 29556 positive class examples (vegetation) and 11404 negative class (non-vegetative) samples. We can see in Figure 2.1 a sample of the first crop, a second crop and an example of the ground truth for the second crop sample .



Figure 2.1: Samples and ground truth

3 | Steps

This project was divided in 3 steps, index extraction, fusion and filtering.

The first step consists of extraction of the 6 selected vegetation indexes, listed below:

1. Normalized green-red difference index

- $\bullet \text{NGRDI} = \frac{G-R}{G+R}$

2. Excess green

- $\bullet \text{ExG} = 2g - r - b$

3. Color index of vegetation

- $\bullet \text{CIVE} = 0.441r - 0.881g + 0.385b + 18.78745$

4. Vegetativen

- $\bullet \text{VEG} = \frac{g}{r^a b^{(1-a)}} \text{ where } a = 0.667$

5. Excess green minus excess red

- $\bullet \text{ExGR} = \text{ExG} - 1.4r - g$

6. Woebbeckindex

- $\bullet \text{WI} = \frac{g-b}{r+g}$

There are several indexes to use in vegetation fraction detection, but some need the Near infra-red (NIR) information, which we don't have. Those six methods were used in [3]. The R, G and B represents the raw value of the red, green and blue component of the pixel and the r,g and b are the normalized values as follow:

$$r = \frac{R}{(R+G+B)}; g = \frac{G}{(R+G+B)}; b = \frac{B}{(R+G+B)}$$

Each index is able to accentuate the green component of the input image and convert from the original RGB space to a grayscale space. They provide a matrix with the same size as the input where each pixel, normalized between 0 and 1, reflects the probability of the pixel being a vegetation.

To find a value capable of separating the vegetation, we build the ROC curve for all images. The ROC curve is built by plotting the True Positive Rate (TPR) against the False Positive Rate (FPR) for different threshold values, whereupon the TPR is the rate of the positive class correctly classified and the FPR is the rate of the miss classified positive class. The ROC curve help to illustrate the discriminating ability of a binary classifier.

The second step is to do tests in order to analyse the index fusion with the Early and Late fusion techniques. The early fusion is based on the combination of indexes to take a decision (vegetation or not). The indexes were combined with the arithmetic and geometric mean [1].

$$\text{ArithmeticMean} = \frac{\sum_{i=0}^N V(i)}{N}$$

$$\text{GeometricMean} = \frac{\prod_{i=0}^N V(i)}{\prod_{i=0}^N V(i) + \prod_{i=0}^N (1 - V(i))}$$

Where N is the number of indexes and V(i) is the vegetation image for the index i.

The late fusion consists of the combination of the decision of each index for the final decision. For this analyses we use the Equal Error Rate (EER) of each index as a threshold for the decision of each pixel and then made a vote (majority choice) to decide whether or not the region is vegetation. The EER is the point where the False Acceptance Rate (FAR) and the False Reject Rate (FRR) are equals, which means that the number of non-vegetation pixel were classified as vegetation(FAR) and the number of vegetation pixel that were classified as non-vegetation(FRR) are the same.

The last step is to apply some filters trying to increase the result. The filters applied was the Bilinear, Gaussian, Mean and Blur. All those filters were chosen with the intent to create a smoother image.

4 | Results

The 6 indexes were extracted from all images and the ROC curve was generated for each index individually and for the early fusion. In Figure 4.2 we can see the difference between the indexes, where a black pixel means non-vegetation and white pixel means vegetation.



Figure 4.1: Example input image

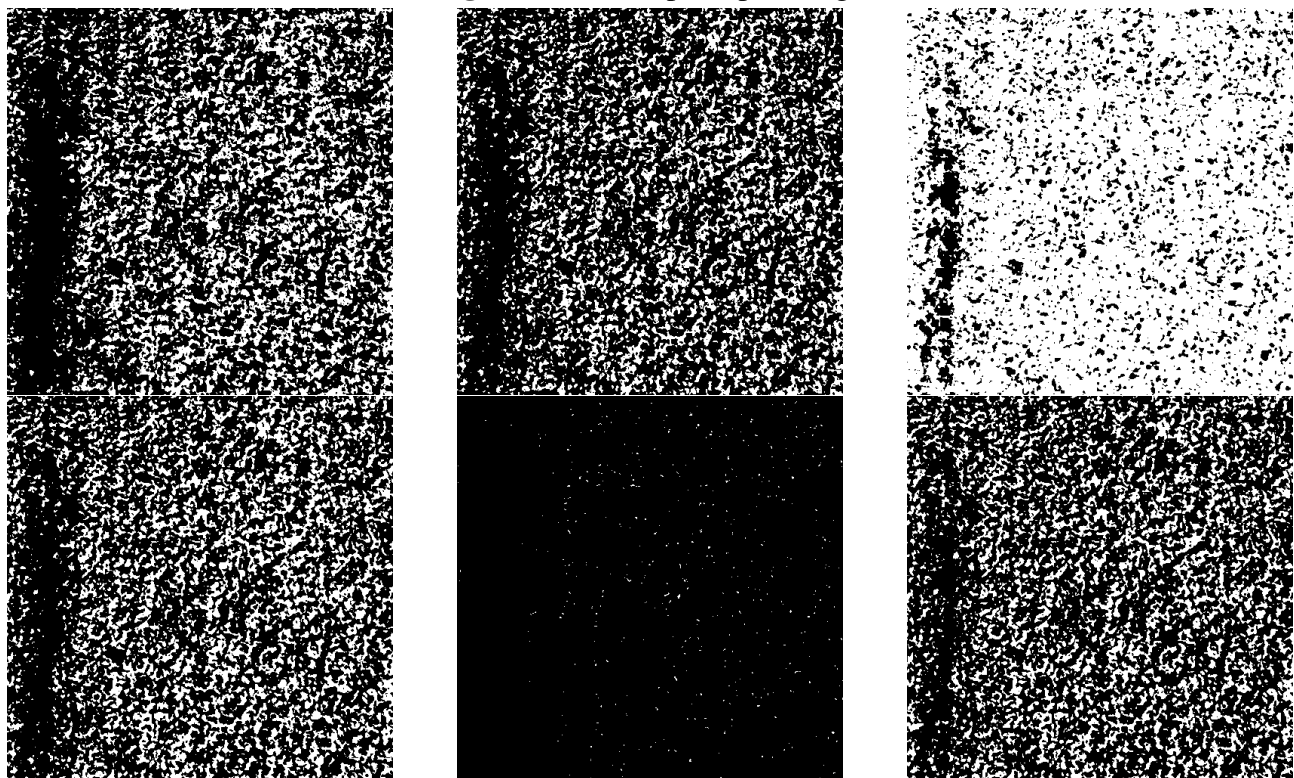


Figure 4.2: Index result for the input example, in order up to right NGRDI, ExG, CIVE, VEG, ExGR and WI

Despite the differences between the indexes, when we apply the process for all input images and plot the ROC, they all have a similar behaviour, as we can see in Figure 4.3 the ROC curve for both crops.

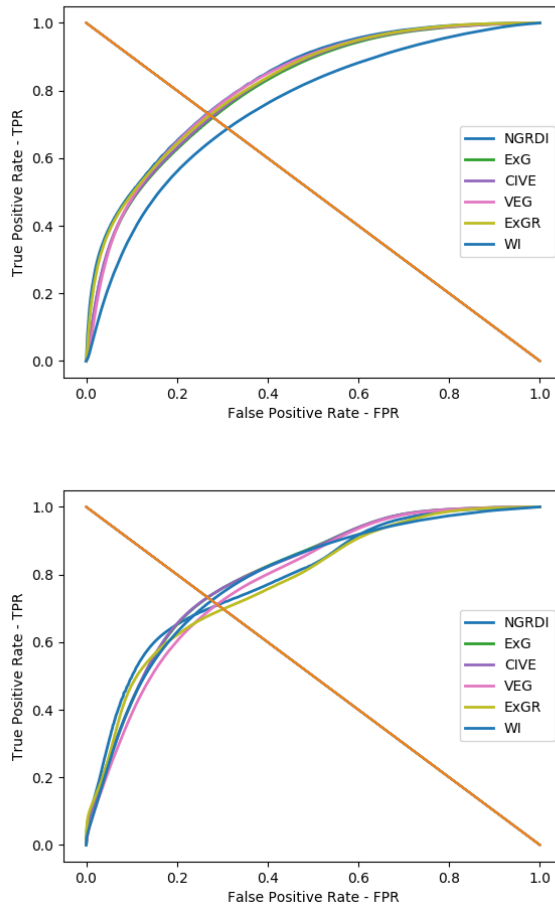


Figure 4.3: ROC Curves

Since they have a similar behaviour, the fusion wasn't expected to give us a big gain. With no filter applied neither the early fusion nor late fusion was capable to improve the accuracy for the first crop, but the late and early fusion give us a better result than the index alone, as show in the accuracy Table 4.1.

Table 4.1: Accuracy crop 1 and 2

Method	Accuracy crop 1	Accuracy crop 2
NGRDI	0.733	0.710
ExG	0.720	0.732
CIVE	0.723	0.732
VEG	0.731	0.711
ExGR	0.727	0.698
WI	0.688	0.723
Arithmetic mean	0.723	0.733
Geometric mean	0.725	0.732
Majority	0.719	0.735

In the next step we apply 4 filters (blur, mean, gaussian and bilinear) and analyse the accuracy. In the Figure 4.4 we can see an input, represented by Figure 4.2, filtered with the blur process and then the NGRDI predictions in Figure 4.5. From the Table 4.2 we can see that the blur was the filter that gave the better performance for the NGRDI index. The blur also was the best filter for all the others indexes.



Figure 4.4: Example of filtered input (Blur, Mean, Gaussian and Bilinear)

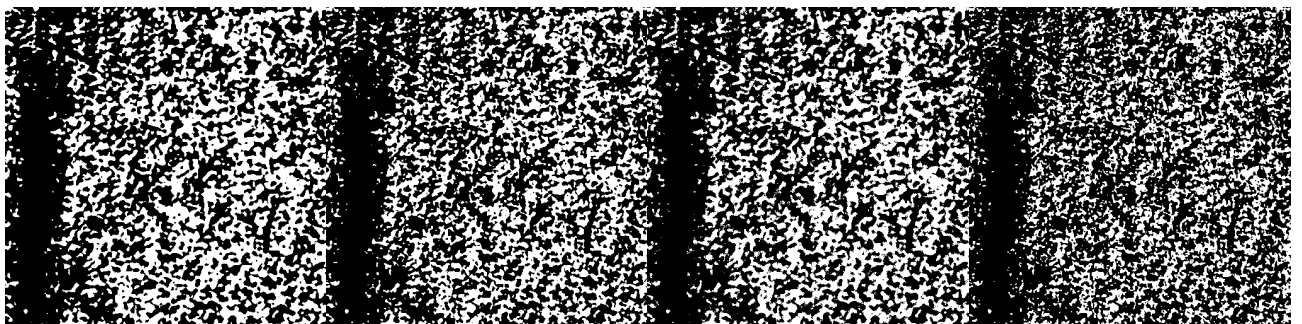
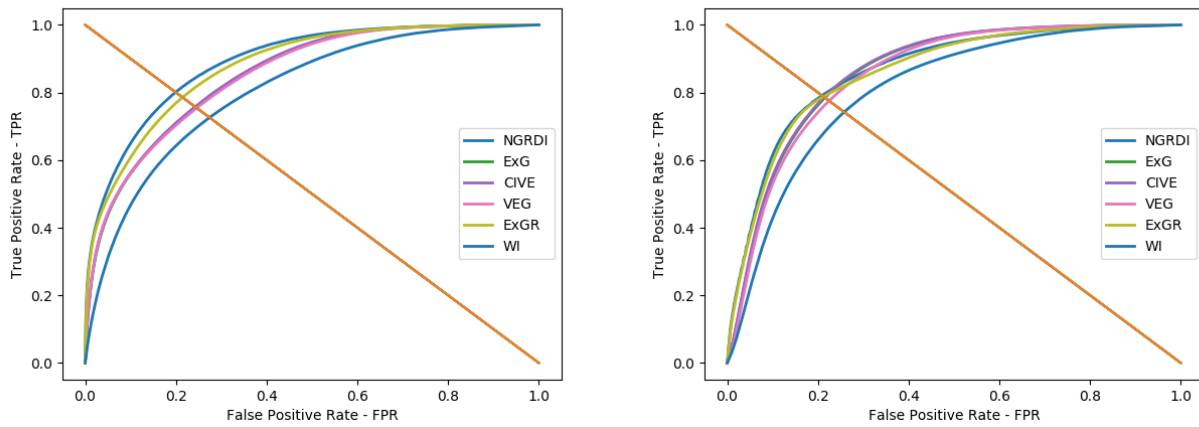


Figure 4.5: NGRDI predictions

Table 4.2: Filter accuracy crop 1 and 2

Filter	Accuracy crop 1	Accuracy crop 2
No filter	0.733	0.710
Blur	0.800	0.791
Gaussian	0.777	0.768
Mean	0.784	0.785
Bilinear	0.736	0.720

Once we found that the blur is the best filter method, we extracted all relevant information about ROC curve for both crops Figure 4.6, like Area Under the Curve (AUC), EER, FAR, FRR and accuracy, represented in Table 4.4.

**Figure 4.6:** ROC curve for blurred input**Table 4.3:** Blurred crop 1 database informations

Method	AUC	EER	FAR	FRR	Accuracy
NGRDI	0.890	0.389	0.199	0.199	0.800
ExG	0.852	0.313	0.243	0.243	0.756
CIVE	0.854	0.313	0.242	0.242	0.758
VEG	0.851	0.287	0.2465	0.246	0.754
ExGR	0.878	0.328	0.214	0.214	0.786
WI	0.804	0.348	0.274	0.274	0.726
Arithmetic Mean	0.862	0.330	0.233	0.233	0.767
Geometric mean	0.862	0.014	0.233	0.233	0.767
Majority					0.759

Table 4.4: Blurred crop 2 database informations

Method	AUC	EER	FAR	FRR	Accuracy
NGRDI	0.865	0.509	0.209	0.209	0.791
ExG	0.861	0.388	0.215	0.215	0.785
CIVE	0.863	0.390	0.214	0.214	0.786
VEG	0.853	0.367	0.225	0.225	0.775
ExGR	0.860	0.462	0.212	0.212	0.788
WI	0.808	0.383	0.258	0.258	0.742
Arithmetic Mean	0.871	0.418	0.206	0.206	0.794
Geometric mean	0.871	0.115	0.206	0.206	0.794
Majority					0.785

References

- [1] Christian Genest and James V. Zidek. *Combining Probability Distributions: A Critique and an Annotated Bibliography*.
- [2] Moacir Ponti, Arthur A. Chaves, Fabio R. Jorge, Gabriel B.P. Costa, Adimara Colturato, and Kalinka R.L.J.C. Branco. *Precision Agriculture with Low Altitude Images using Low Cost Acquisition Systems*.
- [3] J. Torres-Sánchez, J.M. Peña, A.I. de Castro, and F. López-Granados. *Multi-temporal mapping of the vegetation fraction in early-season wheat fields using images from UAV*.
- [4] Naiqian Zhang, Maohua Wangb, and Ning Wanga. *Precision agriculture—a worldwide overview*. 2002.